

FINITE ELEMENT ANALYSIS OF EDDY CURRENTS PROBLEM SUBJECT TO CONVECTIVE DIFFUSION EQUATION

Tatsuya Furukawa* Kokichi Ogawa** Sakutaro Nonaka***

* Saga University, 1 Honjo-machi, Saga, 840 Japan

** Oita University, 700 Dannoharu, Oita, 870-11 Japan

*** Kyushu University, 6-10-1 Hakozaki, Higashi-ku, Fukuoka, 812 Japan

Abstract- The electromagnetic phenomena in the MHD devices, linear induction machines and the transportation of carriers in plasma and semiconductors are subjected to the convective diffusion equation. To solve the equation by numerical methods has recently become of a great importance. The paper presents the FEM analysis of linear induction machines assuming that the field quantities have reached the steady state.

INTRODUCTION

Convective diffusion equation will appear in the hydrodynamic, aerodynamic and various transport phenomena. For example, in the electrical engineering, the electromagnetic fields of MHD generators and linear induction motors (LIMs) are subjected to the equation. Since it contains the Lagrange derivative or substantial derivative, the finite element method (FEM) has been hardly applied to the analyses of the MHD generators and LIMs owing to the asymmetric nature of the stiffness matrix. Some authors [1]-[4] reported the FEM analyses of the stationary or very low-speed LIM, in which the significant convective term [5] may not play a great roll at all but the diffusion term is dominant, that is, the serious end effect [6] can not exist. However, no studies on the high-speed LIMs have not been published yet. In the present paper, we shall introduce the FEM analysis of eddy currents problem subject to the convective diffusion equation based on the complex representation of field quantities. Also we shall show the field calculations of the low- and high-speed LIMs with the single-layer winding[6].

CONVECTIVE DIFFUSION EQUATION AND DISCRETIZATION

The convective diffusion equation, which appears in the LIM, is expressed in the following form in the xz -two-dimensional plane as shown in Fig. 1.

$$\frac{\partial}{\partial x} \left(\nu \frac{\partial}{\partial x} A_y \right) + \frac{\partial}{\partial z} \left(\nu \frac{\partial}{\partial z} A_y \right) = -J_e + \sigma \left(\frac{\partial}{\partial t} + v_2 \frac{\partial}{\partial x} \right) A_y \quad (1)$$

where A_y is the magnetic vector potential, v_2 is the secondary cruising speed, ν is the reluctivity, σ is the conductivity, and J_e is the external supply-current density. In equation (1), the effect of the eddy currents due to the gradient of the electrostatic scalar potential, i.e., $-\nabla\phi$, do not appear explicitly but is approximately taken account of by the conductivity multiplied by the correction factor[7] implicitly.

Suppose that the transient in time ceases and all the electromagnetic quantities vary sinusoidally at an angular frequency ω_1 , the time derivative is replaced with $j\omega_1$, where the j is imaginary unit.

$$\frac{\partial}{\partial x} \left(\nu \frac{\partial}{\partial x} \dot{A}_y \right) + \frac{\partial}{\partial z} \left(\nu \frac{\partial}{\partial z} \dot{A}_y \right) = -\dot{J}_e + \sigma (j\omega_1 + v_2 \frac{\partial}{\partial x}) \dot{A}_y \quad (2)$$

In the last equation, the variables with the dot denote the complex quantities.

Assuming that all the quantities vary linearly in the triangular sub-domains, where the basis functions are the piecewise linear approximations, say, $[N_1, N_2, N_3]$, the vector potential within each element is expressed as a linear interpolation of its values at the three vertices, that is,

$$\dot{A}_y^e(x, z) = [N_1, N_2, N_3] [\dot{A}_1^e, \dot{A}_2^e, \dot{A}_3^e]^T \quad (3)$$

where the subscripts refer to the three vertices, or nodes, and

$$N_i = \frac{1}{2\Delta_e} [(x_j - x_k)z + (z_j - z_k)x + (x_k - x_j)z] \quad (4)$$

$$= a_i + b_i x + c_i z$$

where Δ_e is an area of the triangle and a cyclic permutation of the indices refers to the other vertices.

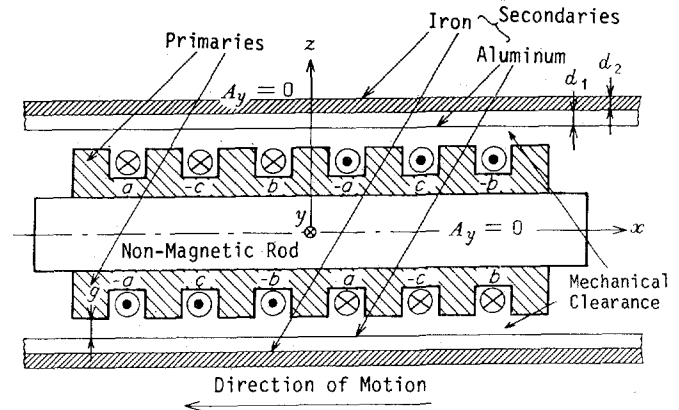


Fig. 1. Model for analysis of tubular LIM.

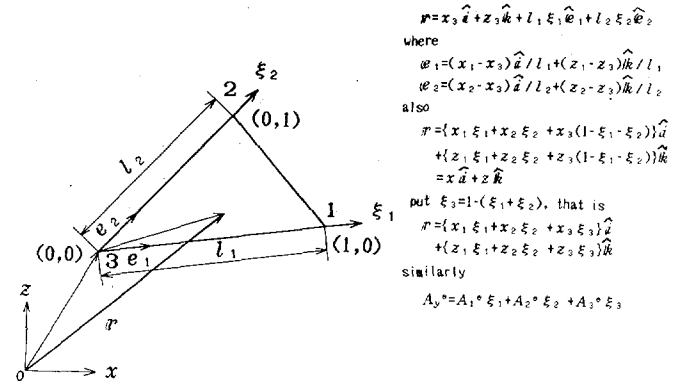


Fig. 2. Local coordinate system.

Applying Galerkin method to (2), the equation may be rewritten as

$$\int \int \int \{ \nu [N_x]^T [N_x] \dot{A}_x + \nu [N_z]^T [N_z] \dot{A}_z + \sigma v_2 [N_x]^T [N_x] \dot{A}_x + j\omega_1 [N]^T [N] \dot{A} + \dot{J}_e [N] \} dx dz = 0 \quad (5)$$

where the subscripts x and z in (5) denote the first order derivative with respect to x and z respectively.

In the last equation, the third term in the in-

tegrand is due to the significant first order derivative [5] in (2), which makes the global stiffness matrix asymmetric. The others are the same as those derived from the regular Poisson's equation. In the present paper, we shall treat the convective term and the transformer term, that is, time derivative one due to the diffusion.

Fig. 2 shows the local coordinate system in one triangular sub-domain, where the origin is set on one of the three vertices. In this case, the point "3" of which coordinate is (x_3, z_3) in the original coordinate system is selected as a new origin.

The position vector r in the domain, which issues from the original origin, is expressed as,

$$r = x_3 \hat{u} + z_3 \hat{k} + l_1 \hat{e}_1 + l_2 \hat{e}_2 \quad (6)$$

where \hat{i} , \hat{k} , \hat{e}_1 and \hat{e}_2 are base in each coordinate system, also \hat{e}_1 and \hat{e}_2 are expressed as,

$$\hat{e}_1 = (x_1 - x_3) \hat{u} / l_1 + (z_1 - z_3) \hat{k} / l_1 \quad (7)$$

$$\hat{e}_2 = (x_2 - x_3) \hat{u} / l_2 + (z_2 - z_3) \hat{k} / l_2 \quad (8)$$

Therefore the r may be rewritten as,

$$r = \{x_1, \xi_1 + x_2, \xi_2 + x_3(1 - \xi_1 - \xi_2)\} \hat{u} + \{z_1, \xi_1 + z_2, \xi_2 + z_3(1 - \xi_1 - \xi_2)\} \hat{k} = x \hat{u} + z \hat{k} \quad (9)$$

If we put $\xi_3 = 1 - (\xi_1 + \xi_2)$, the position r is finally rewritten as,

$$r = (x_1, \xi_1 + x_2, \xi_2 + x_3 \xi_3) \hat{u} + (z_1, \xi_1 + z_2, \xi_2 + z_3 \xi_3) \hat{k} \quad (10)$$

Similarly we can obtain the another expression of (3) in the sub-domain as,

$$\hat{A}_j^*(x, z) = [\xi_1, \xi_2, \xi_3] [\hat{A}_1^*, \hat{A}_2^*, \hat{A}_3^*]^T \quad (11)$$

Consequently the N_i in (3) becomes as follows,

$$[N] = [\xi_1, \xi_2, \xi_3] \quad (12)$$

also

$$[N]^T [N_x] = [\xi_1, \xi_2, \xi_3]^T [b_1, b_2, b_3] / 2\Delta, \quad (13)$$

$$[N]^T [N] = [\xi_1, \xi_2, \xi_3]^T [\xi_1, \xi_2, \xi_3] \quad (14)$$

To evaluate the integrand for the convective and the transformer terms by the Gaussian 7 points numerical integration, the required equations with integrated coefficients for three nodes in each mesh will be written as,

$$\sum_{r=1}^7 \sigma \left\{ j \omega_r w_r \left| \begin{array}{ccc} \xi_1^r \xi_1^r & \xi_1^r \xi_2^r & \xi_1^r \xi_3^r \\ \xi_2^r \xi_1^r & \xi_2^r \xi_2^r & \xi_2^r \xi_3^r \\ \xi_3^r \xi_1^r & \xi_3^r \xi_2^r & \xi_3^r \xi_3^r \end{array} \right| \right. \\ \left. + \frac{v_z}{2\Delta} w_r \left| \begin{array}{ccc} b_1 \xi_1^r & b_2 \xi_1^r & b_3 \xi_1^r \\ b_1 \xi_2^r & b_2 \xi_2^r & b_3 \xi_2^r \\ b_1 \xi_3^r & b_2 \xi_3^r & b_3 \xi_3^r \end{array} \right| \right] \hat{A}_j^* \quad (15)$$

where ξ_j^r s are the seven distinct points in the integrated interval and w_r s are weights.

Assembling all the stiffness matrices of all elements, we can obtain the following global equations in matrix form.

$$[\hat{S}] [\hat{A}] = [\hat{J}] \quad (16)$$

where $[\hat{S}]$ is the global stiffness matrix, $[\hat{A}]$ are unknown potentials and $[\hat{J}]$ includes the external supply-currents. Here the global stiffness matrix exhibits the band structure but contains the asymmetric components such as (15).

Odamura[4] used the upwind Galerkin method[5] and the Crank-Nicolson procedure to introduce the artificial viscosity coefficient for the sake of the convergence of the oscillatory iterated values, however, the

merit of his method has not been found in such his very low-speed LIM. Besides its programming is not so easy because of the introduction of such an artificial coefficient.

The merit of our method is straightforward in view of assembling the global matrix and the results are sure to be stable in time. Though the demerit is that the more memories should be necessary for computations, such a demerit can be overcome by adopting the asymmetric band matrices method together with the Gaussian elimination one. Also the present FEM procedure is available on the micro-computer systems with the smaller memories.

FLUX DISTRIBUTIONS OF LOW- AND HIGH-SPEED LIMs

All computations were performed on the 16-bits micro-computer systems (8086 CPU and 8087 NDP) with 640 KB main memories and 1920 KB memory disk. When the Gaussian elimination procedure can be applied to the global equations taking account of the asymmetric band matrices, we can assure the satisfactory high speed and high precision for calculations in spite of using the micro-computer systems.

(1) Low-speed tubular LIM

Fig. 3 shows the flux distributions of the low-speed tubular LIM (synchronous speed of 39 km/h) with a ring-winding or single-layer winding[6] at the slips of 1.0, 0.5 and zero. It is assumed that the LIM travels in the composite metallic tube (inner aluminum tube, outer iron one) as shown in Fig. 1 and the magnetic saturation can not occur owing to the larger air gaps. The number of nodes necessary for computations was 752.

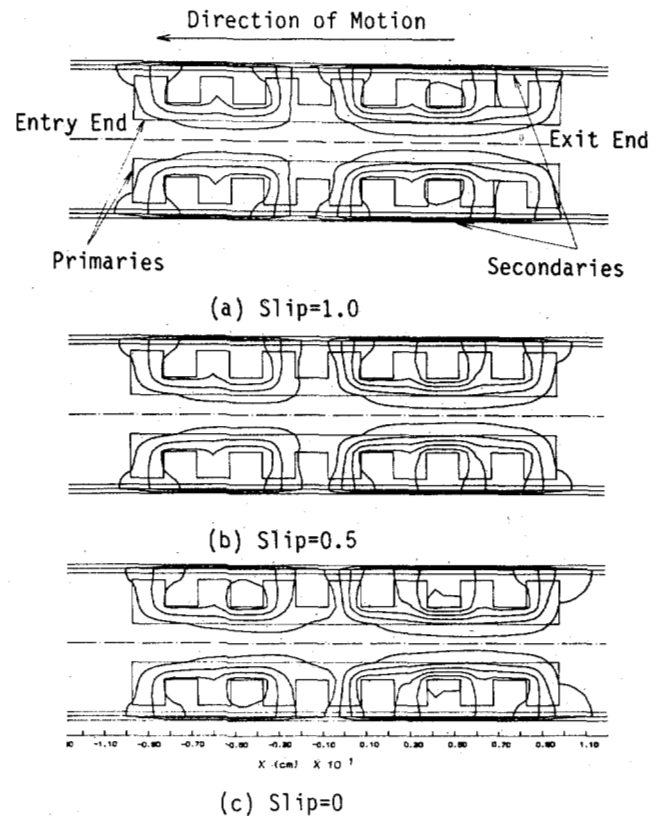


Fig. 3. Flux distributions of low-speed tubular LIM.

Since the stationary pulsating mmf[6] always exists in the single-layer winding, each field is perturbed considerably and the leakage flux from the backs and both the ends of the primary cores is observed.

In the yoke portions of the primaries and the back iron cores of the secondaries, the magnetic flux density becomes less than 1.0 [T]. Therefore it is justified that the magnetic saturation can not occur.

At the slip of zero, the eddy currents due to the end effect decay gradually to be carried out downstream and produce the drag force at the exit end.

(2) High-speed DLIM

Fig. 4 shows the flux distributions of the high-speed double-sided LIM (for short, DLIM, synchronous speed of 494.2 km/h) with a single-layer winding at the slips of 0.5, 0.1 and zero. The number of nodes necessary for computations was 1560.

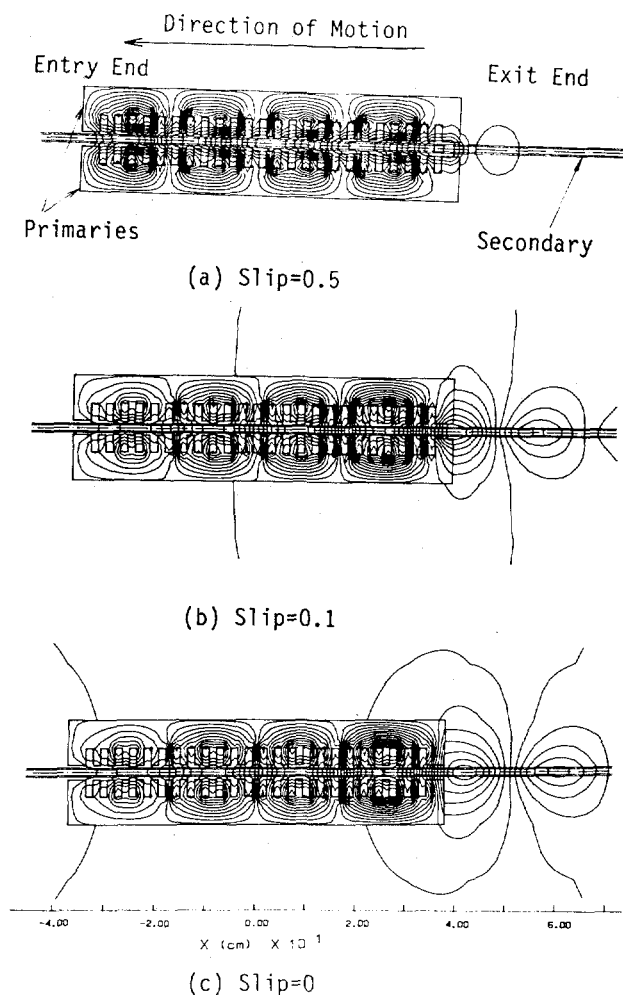


Fig. 4. Flux distributions of high-speed DLIM.

When the LIM has a hollow aluminum secondary conducting plate [8] with 3 mm thickness webs and 10 mm hole width, at the slip of 0.5, the secondary eddy currents, of which slip frequency becomes higher (in this case, 220 Hz), suppress the alternating flux produced by the stationary pulsating mmf as stated.

On the other hand, at the slips of 0.1 and zero (synchronism), the serious end effect is brought about to distort the fields. The leakage flux can be seen out of the backs and both the ends of the primary cores.

The eddy currents due to the end effect wave are carried away downstream to produce the considerable drag forces at the exit end zone. Also the end effect at the lower slip is remarkable in the entry end zone to prevent the magnetic field at the zone from building-up.

CONCLUSIONS

The paper has demonstrated that the FEM of eddy currents problem subject to the convective diffusion equation, when the sinusoidal changes in time occur, is readily applied to the numerical analysis of low- and high-speed LIMs only if the asymmetric band matrices method is incorporated into Gaussian elimination procedure. Also the method is available on the micro-computer systems with the smaller main memories.

ACKNOWLEDGMENT

The authors wish to thank Prof. I. Muta of Saga University for his financial support and Mr. K. Komiya, a graduate student of Saga University, for the preparation of the manuscript.

REFERENCES

- [1] A. Foggia, J. C. Sabonnadiere and P. Silvester, "Finite element solution of saturated travelling magnetic field problem", *IEEE Trans. PAS.*, vol. PAS-94, no. 3, pp. 866-871, May/Jun. 1975.
- [2] J.H.H. Alwash and J.A.H. Al-Rikabi, "Finite-element analysis of linear induction machines", *Proc. IEE*, vol. 126, no. 7, pp. 677-682, Jul. 1979.
- [3] J. Penman, B.J. Chalmers, A.M.A. Kamar and R.N. Tuncay, "The performance of solid steel secondary linear induction machines", *IEEE Trans. PAS.*, vol. PAS-100, no. 6, pp. 2927-2935, Jun. 1981.
- [4] M. Odamura, "Upwind finite element solution for saturated travelling magnetic field problems", *Trans. IEE Japan*, vol. 105-B, no. 7, pp. 613-619, Jul. 1985.
- [5] I. CHRISTIE, D.F. GRIFFITHS, A.R. MITCHELL, and O.C. ZIENKIEWICZ, "Finite element methods for second order differential equations with significant first derivatives", *Int. Jour. Num. Meth. Eng.*, vol. 10, No. 6, pp. 1389-1396, Nov./Dec. 1976.
- [6] S. Nonaka and T. Furukawa, "An analytical problem of conventional LIM theories based on a sinusoidal primary current sheet model with finite length.", *Elect. Eng. Japan*, vol. 104, no. 5, pp. 92-100, Sep./Oct. 1984.
- [7] S. Nonaka and K. Yoshida, "Equivalent circuits for double-sided linear motors", *Elect. Eng. Japan*, vol. 90, no. 3, pp. 32-41, May/Jun. 1970.
- [8] S. Nonaka, N. Fujii and N. Shinoda, "Experimental study on effect of hollow aluminum reaction rail for high-speed LIM", *Elect. Eng. Japan*, vol. 99, no. 4, pp. 80-88, Jul./Aug. 1979.